MODELING AND SIMULATION OF THE ELECTRIC ARC FURNACE FOR THE CONTROL DESIGN PURPOSES

Vito Logar, Dejan Dovžan, Igor Škrjanc

University of Ljubljana, Faculty of Electrical Engineering
1000 Ljubljana, Tržaška 25, Slovenia

vito.logar@fe.uni-lj.si(Vito Logar)

Abstract

Steel is one of the most universal and widely used materials, for which there is yet no suitable substitution. It is produced in two main routes: the ore base route and the scrap based route. The second route is becoming increasingly important, due to large quantities of available scrap metal and today represents more than 1/3 of the world's annual steel production. Therefore, the operation of the electric arc furnace (EAF), which is used to melt the scrap and the melting process also represent an interesting technical, economic and ecologic research field. The main idea of the EAF is to use the heat, which is dissipated from the electric arcs to melt the steel loaded in the baskets. Therefore, in this paper we present an approach to mathematical modeling of the electric processes in an AC EAF, which represent the most critic, complex and very important part of the whole EAF model, which further consist of several energy balance and chemical processes. The presented model is obtained according to different mathematical, physical and electrical laws. The parameters, which are needed to correctly identify the melting process have been fitted experimentally using the measured data of an 80MVA AC furnace operation. Similar data has also been used for the model validation in different operating situations. The aim of the EAF modeling is to obtain a reliable mathematical model of the scrap melting process, which shall further be used for control design purposes and optimization of the energy consumption.

Keywords: Dynamic Model, Electric arc furnace, EAF, Modeling

Presenting Author's Biography

Vito Logar received his B.Sc. and Ph.D. degrees in electrical engineering from the Faculty of electrical engineering, University of Ljubljana, Slovenia in 2004 and 2009, respectively. His research interests include modeling and identification in neurophysiological systems, advanced brain-wave analysis and modeling of the industrial processes.

1 Introduction

In this paper an approach to mathematical modeling of a three-phase AC electric arc furnace (EAF) melting process and operation is investigated. Since the EAF-recycled scrap metal represents 1/3 of the annual steel production and the typical EAF energy consumption is approximately 450kWh/ton of melted steel, the EAF operation and it's processes (electrical, chemical, mechanical, etc.) represent an interesting research field from the technical, economical and ecological point of view. Therefore, the aim of the EAF modeling is to obtain a reliable mathematical model of the melting process, which shall further be used for control design purposes, energy consumption optimization and training the EAF operators by means of the EAF simulator.

The process of scrap refining can be divided into three main steps: 1. loading the baskets with different types of scrap metal; 2. melting the scrap by means of the AC arcs and addition of different additives to attain the desired chemical composition of the steel; 3. tapping of the melted steel and further processing. In this study special attention is devoted to step 2, i.e. melting period of the EAF operation, as it represents the most crucial and complex phase in the EAF operation. The idea of the EAF melting is to transform the electrical energy to thermal energy, which is dissipated from the electric arcs to melt the raw materials loaded in the baskets. The arcs burn between the graphite electrodes and the conducting scrap through the ionized air, which is characterized by low voltages (approx. 400-1000V per phase) and high currents (approx. 40-60kA per phase). The temperatures in the arc's core rise up to 8500K at which the gas discharge holds the electric conductivity of approximately 10^3 S/m. In this manner, melting the scrap is done reasonably fast and efficient.

Model of the EAF and fitting of the parameters has been done for the actual 80MVA AC furnace. For this reason operational data of the EAF during different operating situations has been collected. Measured signals included various electrical (powers; voltages; currents; power factors; stability indexes; operating resistances and reactances; etc.) and other values (transformer and reactor taps; current basket; current heat; number of short circuits and arc breakages; tap-to-tap times; temperature of the cooling panels; composition and weight of the added additives; consumption of oxygen, carbon, gas; etc.) during a normal operation of the EAF.

At this stage of modeling only the electrical values were used for developing the EAF electric circuit model, as they are fairly independent from the other EAF submodels.

2 Measurements and methods

2.1 EAF operation data

For the needs of this study we performed EAF measurements during the melting process in different operational situations. Data which was measured during the melting process included the measurements of the effective values, i.e. root mean squares (RMS), averaged over a 30-second sample-time window of the following: secondary phase voltages; arc voltages; phase currents; power factors; arc resistances and reactances; total resistances and reactances; apparent, active, reactive and arc power; total energy consumption; etc. Furthermore, the information about the total number and mean times of short circuits and arc breakages was also available.

2.2 Methods

There are many possible ways and software tools that can be used to model the EAF processes. In this study we used harmonic analysis in combination with discrete simulation. Therefore, the transformer voltages, which are actually the only electrical input to the model can be described by Eq. 1:

$$U = U_{tap} e^{1 \cdot j 2\pi f t - \frac{\pi}{2}}, \tag{1}$$

where U_{tap} denotes the transformer voltage amplitude, f represents the network frequency ($50Hz$) and t represents the time. In order to obtain the voltages for other two phases the phase angle in Eq. 1 should be rotated by $2\pi/3$ and $4\pi/3$. In this manner, all other electrical values inherit the complex characteristics.

The simulation was performed in *Matlab*'s discrete space with a fixed-step size of $10^{-4}s$. The reason for choosing harmonic analysis over *Simulink-Simscape* for instance, is that discrete simulation implemented by a *Matlab* script runs significantly faster and thus allows real-time experimenting, which crucial when developing a training simulator.

3 Mathematical model

The main part of the AC EAF represents the furnace transformer, which is connected to the 110 - 35kV distribution station via the 19.3MVA furnace reactor. Rated power of the transformer is 80MVA, with secondary voltage range from 600 - 980V divided in 18 steps (transformer taps). Rated current on the primary side extends from 1.060A to 1.320A and from 47kA to 62kA on the secondary side. Allowable 2s short-circuit currents range up to 16kA on the primary and 900kA on the secondary side. Fig. 1 shows the schematic representation of the EAF's electric circuit.

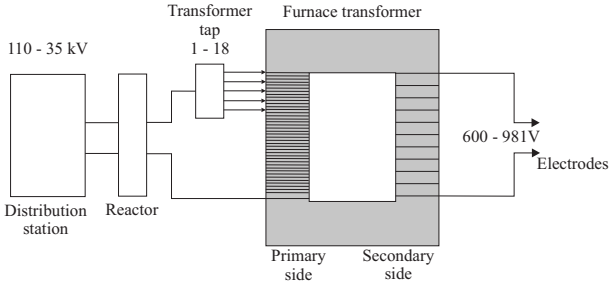

Fig. 1 Schematically presented electric circuit of the 80MVA EAF

The furnace reactor represents a variable reactance load from 3.89 to 0 $m\Omega$ divided into 6 steps (reactor taps),

which is used to increase the circuit reactance in the initial phase of the meltdown process. The purpose of increased reactive load is to raise the stability of the AC arcs, which are due to solid steel and chaotic conditions in the EAF highly unstable and often extinguish.

The electrical model of the EAF can be described as a non-linear 3-phase electric circuit, whose main non-linearities are represented by the electric arcs. Mathematically, the electric arc can be described as an impedance load, whose resistance R_a can be modeled by means of the well-known Cassie-Mayr model [1, 2, 3] from Eq. 2. Due to possible numerical problems, arc resistance R_a is usually expressed in a logarithmic form (s).

$$\frac{ds}{dt} = \frac{1}{\tau}(1 - \frac{U_a I_a}{P_0} exp(\alpha s));\ s = \ln R_a, \quad (2)$$

where R_a represents the arc resistance, U_a represents the arc voltage, I_a represents the phase current, α represents the Cassie-Mayr constant ($\alpha = 0$ - Mayr model for low current values, $\alpha = 1$ - Cassie model for high current values), τ represents the cooling constant of the arc and P_0 represents the arc's power dissipation, described by Eq. 3:

$$P_0 = 2\pi^{1/2}\sigma^{-1/2} l^{3/2} \sigma_{SB} T^4, \quad (3)$$

where σ represents the specific conductivity of the ionized air, σ_{SB} represents the Stefan-Boltzmann constant, l represents the arc length and T represents the arc-core temperature. Eq. 3 and the time constant τ in eq. 2 define the time, which is needed to heat the ionized air (arc) for the current to reach it's steady state $U_a I_a = P_0$ [4].

The arc's reactance X_a can be described by means of the Köhle model [5] in Eq. 4:

$$\frac{X_a}{X_0} = K_1 \frac{R_a}{X_0} + K_e(K_2 \frac{R_a}{X_0} + K_3 \frac{R_a^2}{X_0^2}), \quad (4)$$

where X_0 represents short-circuit reactance, coefficients K_1, K_2 and K_3 represent the dependence of X_a from the resistance R_a, while the parameter K_e, can be described by Eq. 5:

$$K_e = e^{-\frac{t}{T_x}}, \quad (5)$$

and describes the exponential decrease of reactance with time. T_x represents a time constant, being in the $10 \ldots 15$ minutes range. The exponential impedance drop is a direct consequence of the scrap melting process. In the initial stage of melting, with no melted steel present the arc's impedance load is high, while it gradually decreases to the lowest value at the end of the melting period (all steel molten - flat bath).

According to Eq. 2 and 4 the arc impedance can be obtained by Eq. 6:

$$Z_a = \sqrt{R_a^2 + X_a^2}, \quad (6)$$

which is a well-known equation for calculating the load's impedance.

According to the literature [6], the arc voltages are reduced for about 30-40V due to the cathode voltage drop, which can be represented as an additional resistance. Therefore, observing Fig. 2, the actual arc impedance Z_{arc} is by $R_{cathode}$ smaller from the Z_a calculated in Eq. 6:

$$Z_{arc} = Z_a - R_{cathode} = Z_a - \frac{U_{cathode}}{I_a}, \quad (7)$$

where $U_{cathode}$ is the corresponding cathode voltage drop.

Therefore, the EAF electric model, including inner transformer impedances, line impedances, arc impedances and media impedances (i.e. scrap, slag impedance etc.) can be represented by a three-phase AC circuit, which is shown in Fig. 2.

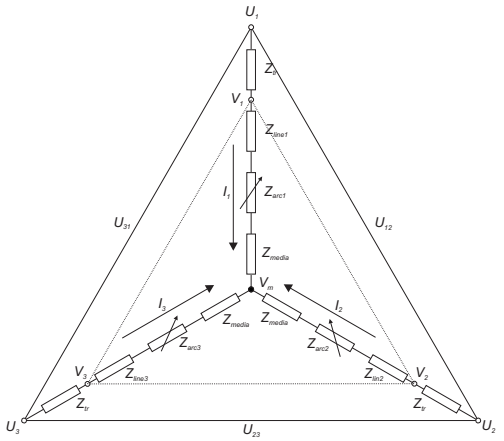

Fig. 2 Electric diagram/model of an EAF; U_1, U_2, U_3 - phase voltages, U_{12}, U_{23}, U_{31} - phase-to-phase voltages, I_1, I_2, I_3 - phase currents, Z_{tr} - transformer and reactor impedance, Z_{line} - line impedances, Z_{arc} - arc impedances, Z_{media} - media impedance, V_m - neutral point potential

According to Eq. 2 and 4 the impedances of the electric arcs represent a non-linear time-variant loads, which consecutively cause an unbalanced furnace operation. Thus, the three-phase free neutral point V_m (which has the potential of 0 when operating with balanced/symetrical furnace load, i.e. constant impedance loads in all phases) moves inside the U_{12}, U_{23}, U_{31} triangle; typically, in a circle with a diameter proportional to arc's impedance Z_a and position on the circle defined by the phase shift of the neutral point potential V_m as to phase-to-phase voltages. V_m reaching the edge of a triangle means that one of the arcs extinguished and needs to be re-ignited. Therefore, the typical unbalanced furnace operation can be represented by a phasor diagram shown in Fig. 3.

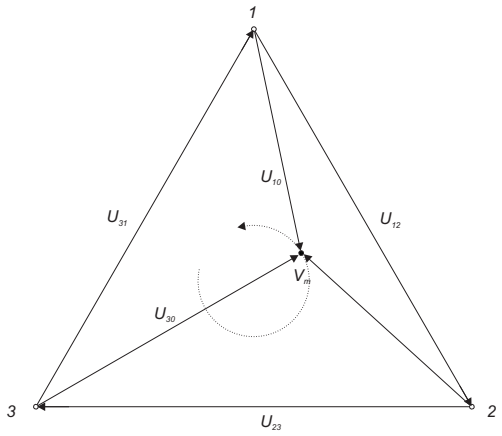

Fig. 3 Phasor diagram of an unbalanced furnace operation; U_{12}, U_{23}, U_{31} - phase-to-phase voltages, U_{10}, U_{20}, U_{30} - phase-to-neutral voltages, V_m - free neutral point potential

The neutral point potential V_m can be determined by Eq. 8:

$$V_m = \frac{\sum_{i=1}^{3} Y_i U_i}{\sum_{i=1}^{3} U_i}, \tag{8}$$

where Y_i represents the sum of phase admittances and U_i represents the phase voltages.

Observing the phasor diagram in Fig. 3 it is clear that changes in either of the arcs have a direct influence on the other two arcs. Whether, one of the arcs should extinguish, the phase-to-neutral voltages of the other two arcs reduce to $1/2$ of the phase-to-phase voltage, which also has a direct influence to the loss of the EAF's total power.

Voltages and phase currents can be computed by means of the Kirchoff's voltage and current laws. Total voltage drop on transmission lines, arc and media can be computed from Eq. 9:

$$V = \frac{(Z_{arc} + Z_{line} + Z_{media}) \cdot (U_1 - V_m)}{Z_{arc} + Z_{line} + Z_{media} + Z_{tr}}, \tag{9}$$

and the phase currents can be obtained from equation Eq. 10:

$$I = \frac{U_1 - V_m}{Z_{arc} + Z_{line} + Z_{media} + Z_{tr}}. \tag{10}$$

The arc's voltage drop can be computed by means of the equation Eq. 11:

$$V_{arc} = I \cdot Z_{arc} - V_{cathode} = I \cdot Z_{arc} - I \cdot R_{cathode}. \tag{11}$$

Total apparent (S), active (P), arc (P_{arc}) and reactive (Q) powers of the EAF can be obtained combining the voltages and currents computed in Eq. 9, 10 and 11 by equations Eq. 12, 13, 14 and 15:

$$S = \sqrt{3} \cdot V \cdot I, \tag{12}$$

$$P = I^2 \cdot (R_{arc} + R_{line} + R_{media}), \tag{13}$$

$$P_{arc} = I^2 \cdot R_{arc}, \tag{14}$$

$$Q = \sqrt{S^2 - P^2}. \tag{15}$$

Power factors for each phase can be obtained by Eq. 16:

$$\cos\varphi = \frac{P}{S}. \tag{16}$$

In order to optimally parameterize the mathematical model and to achieve the optimal match between the measured and the simulated data, appropriate values for the following parameters should be obtained: Z_{media} - media impedance; $V_{cathode}$ - cathode voltage drop; K_1, K_2, K_3 - arc reactance/resistance coefficients; T - arc-core temperature; σ - arc conductivity; τ - arc cooling constant and T_x - time constant for R_a to X_a ratio.

The above mentioned parameters were fitted experimentally, observing the real and simulated data and altering the relevant parameters to obtain satisfactory response of each submodel. Furthermore, since the melting process exhibits excessive chaotic behavior, which cannot be modeled by conventional electric laws, a form of randomness needs to be added to the existent mathematical equations. Thus, Lorentz attractor has been added as noise to the length/resistance of the electric arcs to achieve greater similarity of simulated and measured data [7]. The Lorentz attractor can be described by Eq. 17:

$$\begin{aligned} \frac{dx}{dt} &= K\sigma(y - x) \\ \frac{dy}{dt} &= Kx(\varrho - z) - Ky \\ \frac{dz}{dt} &= Kxy - K\beta z, \end{aligned} \tag{17}$$

where K denotes the frequency of the attractor (set to $K = 55$), σ, ϱ and β represent the attractor parameters (set to $\sigma = 10$, $\varrho = 58$ and $\beta = 8/3$) and x, y, z represent the attractor states. Therefore, the resistance of the arcs is altered by adding the randomness of the attractor, as described by Eq. 18

$$R_{arc} = R_{arc} + (x+y+z) \cdot K_t - \overline{(x+y+z)} \cdot K_t, \tag{18}$$

where K_t represents the time-variant attractor gain (larger in the beginning of melting), and $\overline{(x+y+z)}$ represents the mean value of the attractor's states (to retain the average value of the R_a).

3.1 Electrode control

Since the aim of this paper is to build a reliable mathematical model for control design purposes and optimization of the energy consumption (similar to [8]), this section deals with a glance overview of the existent electrode control structure and an approach to it's modeling.

Electrode control can be considered as the only real control-related system (except the auxiliary systems) of the EAF and therefore represents a very important part of it's operation, since the position of the electrodes directly influences the length of the arcs and consequently their resistance. The length of each arc is together with the momentary EAF settings (transformer tap, reactor tap) important because it affects the arc's power. Usually, at the beginning of each heat the EAF operates with lower secondary voltages and short arcs (lower arc resistance) due to highly unstable furnace operation as a consequence of solid steel. Also, the lack of molten steel and slag exposes the arcs, whose high thermal radiation damages the furnace walls. When the electrodes bore themselves into the steel, the EAF operator rapidly increases secondary voltages, which allow melting with longer arcs (higher resistance) and higher arc powers. When quantities of steel large enough are completely molten the furnace power is decreased to maintain the preferred bath temperature for adding various supplements.

The aim of electrode control is to efficiently track the predefined operation set-points. Control structure is based on three univariable PID controllers for each phase/arc separately. At the beginning of the EAF operation the set-points/references are defined with arc resistances. When the resistance set-points are approximately reached the control algorithm switches the set-points/references from arc resistances to EAF active power. Thus, further EAF operation is controlled by arc's active power. Electrode positioning is done by means of a hydraulic system.

At this point the hydraulic system has not been modeled yet; therefore, a reasonable substitution of a first order system has been used with all the appurtenant limitations of the hydraulic system. The main limitation of the hydraulics is the maximum electrode movement speed, which is limited to 10cm/s (25cm/s in case of a short circuit). Considering the dynamics of the hydraulics and the approximate model used, no major deviations between those two are expected.

4 Results

The following section presents the simulation results obtained from the presented mathematical model in comparison with the measured EAF data. The validation of the model is done for one heat (3 baskets) with different transformer taps. Figures 4 to 9 show the comparison between the measured and the simulated data for the EAF's arc resistances and reactances, powers (apparent, active, arc and reactive) and power factors for all three phases.

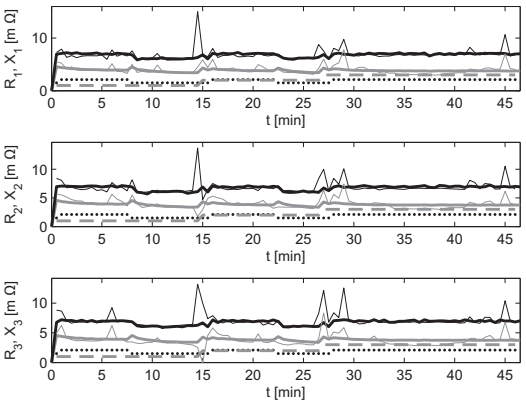

Fig. 4 Arc resistance and reactance in $m\Omega$ for each phase; dotted line - current basket, dashed line - current transformer tap, darker thin line - measured data (resistance), darker thick line - simulated data (resistance), lighter thin line - measured data (reactance), lighter thick line - simulated data (reactance)

Observing Fig. 4 it can be seen that arc reactances raise each time when a new basket of steel is loaded into the furnace and then exponentially decrease to a certain stationary value. This is due to loading the solid steel, which increases the arc instability and consequently it's reactance. Reactance decrease is a direct consequence of steel passing from solid to liquid state. As also presented by Fig. 4 it is obvious that simulated and measured data well-match, which indicates the adequacy of the given submodel.

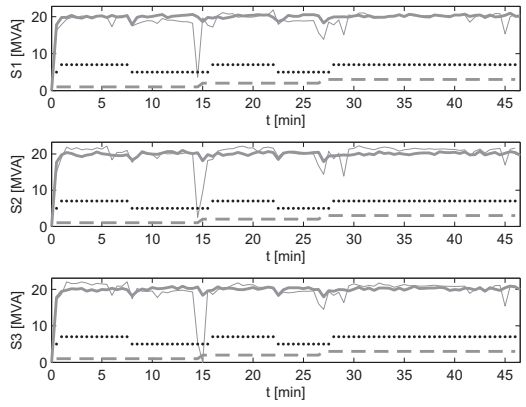

Fig. 5 Total apparent power in MVA for each phase; dotted line - current basket, dashed line - current transformer tap, thin line - measured data, thick line - simulated data

Fig. 5 shows that the furnace operates with approximately 20-22MVA per phase. Total apparent power of the furnace could be raised to use the full potential of the furnace transformer (80MVA); however, the power is normally set according to the optimal time/cost diagram.

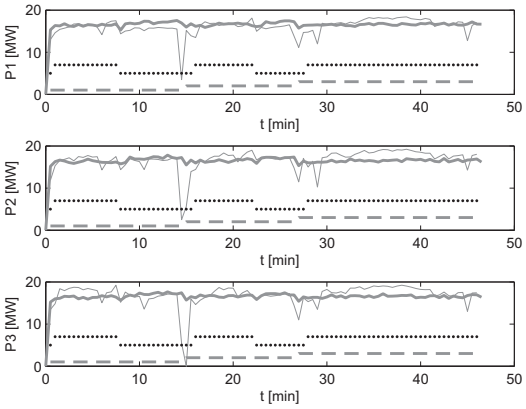

Fig. 6 Total active power in MW for each phase; dotted line - current basket, dashed line - current transformer tap, thin line - measured data, thick line - simulated data

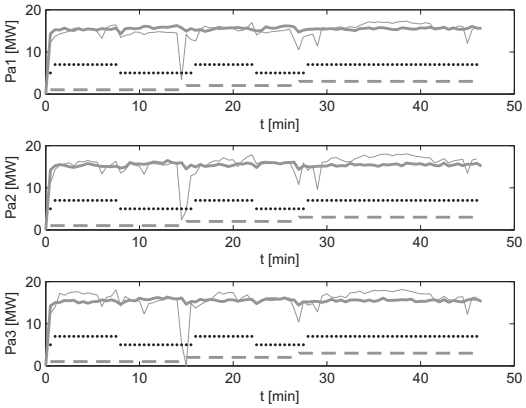

Fig. 7 Total arc power in MW for each phase; dotted line - current basket, dashed line - current transformer tap, thin line - measured data, thick line - simulated data

As can be seen from Fig. 6 to 8 the submodels for active, arc and reactive powers also output data which is adequate to the obtained measurements. It can be seen that the furnace operating with approximately 20-22MVA uses only 15-17MW of active power (arc) to melt the scrap. The loss of power occurs due to inner transformer and line impedances, cathode voltage drops and additional reactive loads (furnace reactor), which stabilize the burning of the arcs but increase the furnace's reactive component (lower power factor).

As can be seen from Fig. 9 the measured and simulated power factors match very well. The furnace is operating with power factors around 0.85 due to relatively high

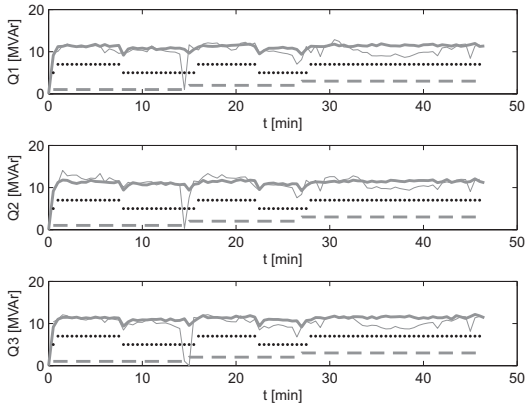

Fig. 8 Total reactive power in MVAr for each phase; dotted line - current basket, dashed line - current transformer tap, thin line - measured data, thick line - simulated data

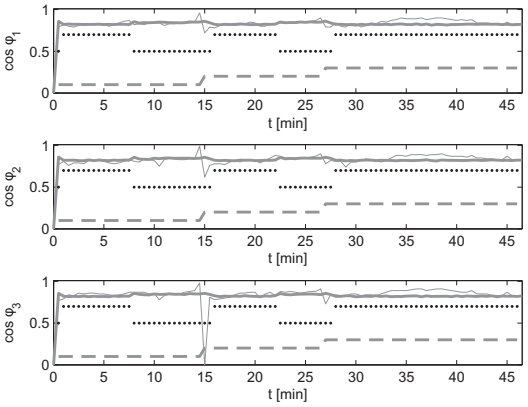

Fig. 9 Power factor for each phase; dotted line - current basket, dashed line - current transformer tap, thin line - measured data, thick line - simulated data

reactive loads, which worsen the active/reactive power ratio, but are associated and dependent on electric characteristics of the arcs and other components.

Since optimization of the energy consumption is one of the main aims for our future work, simulated and measured data should be nearly identical. The result of total energy consumption (measured and simulated) is shown in Fig. 10.

As can be seen from Fig. 4 to 10 comparing the measured and the simulated EAF data, the proposed mathematical approach accurately models the behavior of the EAF in different operational situations. Therefore, the validation of the proposed model can be considered as successful. Also, additional noise added by Lorentz attractor contributes to greater similarity and realism of the computed outputs, when compared to the real-time EAF measurements.

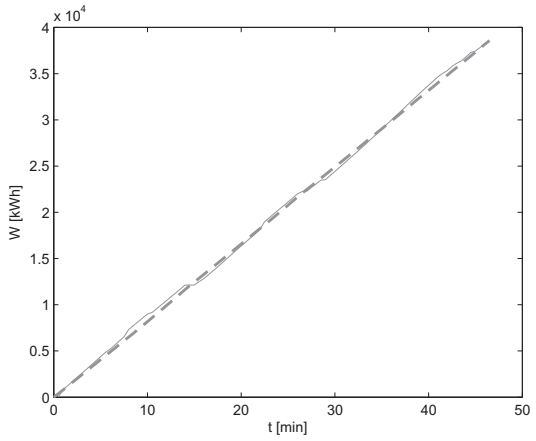

Fig. 10 Total energy consumption in kWh per heat; thin line - measured data, dashed line - simulated data

5 Conclusion

In this paper an approach to mathematical modeling of the EAF is presented. Observing the presented results it can be concluded that the developed model gives satisfactory results, since it accurately follows the data measured during an actual EAF operation in different operational situations.

The presented modeling approach so far represents the first step in the complete EAF modeling project. The presented model already allows testing of various control structures to certain extent; however, in order to use it's full potential and to use it for energy consumption optimization additional models (thermal, energy balance, chemical) shall be built in the near future. Nevertheless, obtaining a reliable electrical model at this stage of the project is crucial, since all other submodels are directly dependent on the electrical characteristics of the electrical model, presented in this paper.

6 References

[1] A. M. Cassie. Arc rupture and circuit severity. Technical Report 102, Internationale des grands Reseaux Electriques a haute tension (CIGRE), Paris, France, 1939.

[2] O. Mayr. Beiträge zur theorie des statischen und dynamischen lichtbogens. *Archiv für Elektrotechnik*, 37:588, 1943.

[3] K. J. Tseng, Y. Wang, and D. M. Vilathgamuwa. An experimentally verified hybrid cassie-mayr electric arc model for power electronics simulations. *IEEE Transactions on Power Electronics*, 12:429–436, 1997.

[4] Y. Lee, H. Nordborg, Y. Suh, and P. Steimer. Arc stability criteria in ac arc furnace and optimal converter topologies. In *22nd Annual IEEE Applied Power Electronics Conference*, pages 1280–1286, 2007.

[5] S. Köhle, M. Knoop, and R. Lichterbeck. Lichtbogenreaktanzen von drehstrom-lichtbogenöfen. *Elektrowärme international*, 51:175–185, 1993.

[6] J. Bratina. *Elektroobločna peč*. Slovenske Železarne, 1994.

[7] G. Jang, W. Wang, G. T. Heydt, S. S. Venkata, and B. Lee. Development of enhanced electric arc furnace models for transient analysis. *Electric Power Components and Systems*, 29:1060–1073, 2001.

[8] R. D. M. MacRosty and C. L. E. Swartz. Dynamic optimization of electric arc furnace operation. AIC*h*E *Journal*, 53:640–653, 2007.